Frequency Regions for Forced Locking of Self-Pulsating Multi-section DFB Lasers

Uwe Bandelow

Weierstrass Institute for Applied Analysis and Stochastics, Mohrenstraße 39, 10117 Berlin, Germany

email: bandelow@wias-berlin.de

Lutz Recke

Humboldt University Berlin, Department of Mathematics, Unter den Linden 6, 10099 Berlin, Germany

email: recke@hu-berlin.de

and

Björn Sandstede

Weierstrass Institute for Applied Analysis and Stochastics, Mohrenstraße 39, 10117 Berlin, Germany

email: sandstede@wias-berlin.de

July 10, 1997

Abstract

A method is developed which allows for the calculation of locking regions of self-pulsating multi-section lasers which are exposed to external optical data sequences. In particular, resonant locking is investigated where both wavelength detuning and detuning of the power frequencies are important.

Classifcation: PACS-1996: 42.55.Px, 42.60.Gd, 42.60.Mi, 42.79.Sz, Keywords:

Frequency Locking, Selfpulsations, Clock Recovery, DFB Lasers, Optical Communication Systems

1 Introduction

In experiments, fast self-pulsations (SP) have recently been discovered in multi-section DFB lasers [2, 3]. These self-pulsations exhibit frequencies from 10 to 80 GHz and are therefore of great technical interest. Within the range of about 10 − 20 GHz, their existence has been attributed in [4, 5, 1] to the dispersive self-Q-switching mechanism (DQS), a single-mode instability. This relation was further corroborated by a detailed comparison of experiment and theory for a 3-section DFB laser [5]. Also, in 1994, the applicability of these SP's for clock recovery has been shown experimentally at 18 GBit/s [6]. Self-pulsations are therefore an important feature for future high-speed data transmission.

The purpose of this paper is an extension of the theory of DQS for free-running single-mode SP's. We are interested in resonant locking of a self-pulsating DFB laser when one facet of the laser is exposed to an external optical signal. It is assumed that the wavelength and the clock frequency of the optical signal are close to those of the free-running laser. The theory presented here will predict regions of the relevant laser and signal parameters for which locking occurs. Finally, the method is applied to self-pulsating states of the 3-section DFB laser studied in [5].

2 Theory

Assuming stable index-guiding of the fundamental transverse TE-mode, the main component of the electric field in a laser can be written as a superposition of a forward and a backward traveling wave [1]

$$E(\vec{r},t) = A(x,y)e^{i\omega_0 t}\left(\psi_+(z,t)e^{-i\frac{\pi}{\Lambda}z} + \psi_-(z,t)e^{i\frac{\pi}{\Lambda}z}\right).$$

Here, Λ is the corrugation period, and ω_0 is a constant optical reference frequency which we choose to be close to the emission frequency of the laser. The transverse field profile $A(x,y)$ of the waveguide can be normalized such that $|\psi_+(z,t)|^2$ and $|\psi_-(z,t)|^2$ are the powers guided by the forward and backward wave, respectively. The time evolution of the amplitudes is governed by the traveling-wave equation

$$i\frac{\partial\psi(z,t)}{\partial t} = -H(z,n(t))\,\psi(z,t) \quad \text{with} \quad \psi = \begin{pmatrix} \psi_+ \\ \psi_- \end{pmatrix} \quad \text{for} \quad 0 \le z \le L, \tag{1}$$

where L is the length of the laser, and $H(z, n(t))$ is a matrix operator given by

$$H = v_g \begin{pmatrix} i\frac{\partial}{\partial z} - (\beta - \frac{\pi}{\Lambda}) & -\kappa \\ -\kappa & -i\frac{\partial}{\partial z} - (\beta - \frac{\pi}{\Lambda}) \end{pmatrix}.$$

Here, v_g is the group velocity, and κ is the coupling coefficient due to the presence of the DFB-grating. Moreover, β denotes the propagation constant at $\omega = \omega_0$, which depends on the longitudinal position z and on the time t via the carrier distribution $n(z,t)$.

For the sake of simplicity, we will work with a spatially averaged number $n_k(t)$ of carriers within the kth section of the laser and apply the same model for β as in [5]

$$\beta_k = \beta_{Ik}\frac{I_k}{L_k} + \beta_{nk}(\frac{n_k}{V_k} - n_t) + \frac{i}{2}(G_k(n_k) - \alpha_{0k}) + \frac{\pi}{\Lambda},$$

using the logarithmic gain model $G_k(n) = g_k' n_t \ln(n/V_k n_t)$. V_k is the active volume of the kth section. The parameters β_{Ik} and β_{nk} are heating and carrier contributions, respectively, to the effective index in terms of β, see [5]. The waveguide absorption is denoted by α_0, and n_t is the transparency density. The dynamics of the carrier numbers is now governed by the balance equation

$$\frac{dn_k}{dt} = \frac{I_k}{e} - \frac{n_k}{\tau_k} - \frac{G_k(n_k)}{\hbar\omega}\langle\psi,\psi\rangle_k, \tag{2}$$

where I_k denotes the injection current of the section S_k, e is the elementary charge and $\hbar\omega \approx \hbar\omega_0$ is the energy of a single photon. In (2), we used the notation

$$\langle\phi,\varphi\rangle_k \equiv \int_{S_k} \left(\phi_+^*(z,t)\varphi_+(z,t) + \phi_-^*(z,t)\varphi_-(z,t)\right)\, dz,$$

for any two-component functions $\phi(z,t), \varphi(z,t)$.[1]

At the facets of the laser, we assume the boundary conditions

$$\psi_+(0,t) = r_0\,\psi_-(0,t) + e^{i\rho t}a(t) \quad \text{and} \quad \psi_-(L,t) = r_L\,\psi_+(L,t), \tag{3}$$

where r_0 and r_L denote the amplitude facet reflectivities, and $a(t)$ is the external signal with optical frequency ρ relative to ω_0. The power frequency of the external signal is denoted by σ, i.e. $a(t)$ is $\frac{2\pi}{\sigma}$-periodic.

[1] If the integral in the above formula is computed over the whole laser length, we will drop the index k. Also, * denotes complex conjugation.

Let $\psi(z,t) = e^{i\rho_0 t}\psi^0(z,t)$ and $n_k(t) = n_k^0(t)$ be a self-pulsating solution of the free-running laser, i.e. $a(t) = 0$, with averaged optical frequency ρ_0 relative to ω_0 and power frequency σ_0. We then seek solutions of (1-3) employing the perturbation ansatz

$$\begin{aligned} \rho &= \rho_0(1 + |a|\rho_1) + O(|a|^2), \\ \sigma &= \sigma_0(1 + |a|\sigma_1) + O(|a|^2), \\ \psi(z,t) &= e^{i(\rho t+\delta)}\psi^0(z, t + \gamma/\sigma) + O(|a|), \\ n_k(t) &= n_k^0(t + \gamma/\sigma) + O(|a|), \end{aligned} \tag{4}$$

where $|a|^2 = \max_{t\in[0,2\pi/\sigma]} |a(t)|^2$ is the maximal power of the optical signal.

We substitute (4) into (1-3) and expand the resulting equation in powers of $|a|$. Upon omitting terms of order $O(|a|^2)$, we then obtain solvability conditions [7]. These conditions depend on solutions (Ψ^j, N_k^j) of the linear system

$$i\frac{\partial \Psi^j}{\partial t} = -(H^*(z, n^0(t)) - \rho_0)\ \Psi^j + 2\psi^0 \sum_k \frac{G_k(n_k^0)}{\hbar\omega}\chi_k(z) N_k^j, \tag{5}$$

$$\frac{dN_k^j}{dt} = \frac{N_k^j}{\tau_k} + \frac{G_k'(n_k^0)}{\hbar\omega} N_k^j \langle \psi^0, \psi^0\rangle_k - v_g \Re e \left(\frac{d\beta_k^*}{dn_k}\langle \psi^0, \Psi^j\rangle_k\right) \tag{6}$$

for $j = 1, 2$ with boundary conditions

$$\Psi_-^j(0,t) = r_0^*\, \Psi_+^j(0,t) \quad \text{and} \quad \Psi_+^j(L,t) = r_L^*\, \Psi_-^j(L,t) \tag{7}$$

subject to the normalization

$$\begin{aligned} \frac{1}{\sigma_0}\int_0^{\frac{2\pi}{\sigma_0}} \left(\Re e \left\langle \Psi^j, \frac{\partial \psi^0}{\partial t}\right\rangle + \sum_k N_k^j \frac{dn_k^0}{dt}\right) dt = \delta_{j1}, \\ -\Im m \int_0^{\frac{2\pi}{\sigma_0}} \langle \psi^0, \Psi^j\rangle\, dt = \delta_{j2}. \end{aligned} \tag{8}$$

Here, H^* denotes the adjoint of the evolution operator H appearing in (1). The function $\chi_k(z)$ appearing in (5) is one for z in the kth section and zero otherwise. If (1-3) with $a(t) = 0$ is linearized about the given self-pulsating solution $(\psi^0(z,t), n_k^0(t))$, then (5-7) is the corresponding adjoint linear system. Furthermore, (8) are bi-orthogonality conditions between the fundamental solutions

$$(\psi(z,t), n_k(t)) = \left(\frac{\partial \psi^0}{\partial t}(z,t), \frac{dn_k^0}{dt}(t)\right) \text{ and } (i\psi^0(z,t), 0)$$

of the linearized equation and the fundamental solutions $(\Psi^j(z,t), N_k^j(t))$ for $j = 1, 2$ of the adjoint equation. We denote the Ψ_--components of the solutions $\Psi^j(z,t)$ of (5-8) evaluated at $z=0$ by $\Psi_-^j(0,t)$.

The solvability conditions mentioned above are then given by

$$\begin{aligned}\Delta\rho &= \rho - \rho_0 = \rho_0\,\Re e\Big(e^{-i\delta}\int_0^{\frac{2\pi}{\sigma_0}} a(t-\frac{\gamma}{\sigma_0})\Psi_-^1(0,t)\,dt\Big),\\ \Delta\sigma &= \sigma - \sigma_0 = \sigma_0\,\Re e\Big(e^{-i\delta}\int_0^{\frac{2\pi}{\sigma_0}} a(t-\frac{\gamma}{\sigma_0})\Psi_-^2(0,t)\,dt\Big).\end{aligned} \tag{9}$$

These are two real-valued nonlinear equations which relate the locked phases γ and δ with the locked optical and power frequencies up to order $O(|a|^2)$. The locking region is given as follows: Upon varying the relative phases δ and γ, the pair $(\Delta\rho, \Delta\sigma)$ will sweep a certain region in the plane. The locking domain in (ρ, σ) can therefore be calculated asymptotically for small maximal input power.

3 Single-mode approximation

It has been shown in [5] that DQS, calculated by the single-mode approximation of (1) developed in [1], is in excellent agreement with the full PDE (1) as well as with experiments. It is therefore reasonable to compute the solutions of the linear system (5-8) using the single-mode approximation rather than the full PDE (1).

Modes are eigenfunctions of the evolution operator H appearing in (1) subject to the boundary conditions (3) with $a(t) = 0$. Let Φ satisfy

$$H(z, n(t))\ \Phi(z, n(t)) = \Omega(n(t))\ \Phi(z, n(t)), \tag{10}$$

normalized according to

$$\frac{2}{L}\int_0^L \Phi_+(z, n(t))\,\Phi_-(z, n(t))\,dz = 1 \tag{11}$$

for all times [4, 1]. Rather than solving equation (1), we will only take the mode with the lowest threshold, i.e. smallest $\Im m(\Omega)$, into account. This is the single-mode approximation [1]. The field amplitudes are then given by

$$\psi = f(t)\,\Phi(z, n(t)), \tag{12}$$

and the evolution of $f(t)$ is governed by

$$\frac{df}{dt} = i\Omega f. \tag{13}$$

Furthermore, equation (2) for the carrier dynamics is given by

$$\frac{dn_k}{dt} = \frac{I_k}{e} - \frac{n_k}{\tau_k} - \frac{G_k(n_k)}{\hbar\omega}|f|^2\langle\Phi,\Phi\rangle_k. \tag{14}$$

Suppose that (13-14) has a self-pulsating solution (f^0, n_k^0). We would like to calculate the locking properties of the laser state (f^0, n_k^0). Recalling the basic strategy which has been explained in the last section, we shall linearize the unperturbed system (13-14) about the self-pulsating solution (f^0, n_k^0). The corresponding adjoint linearized system is then given by

$$\frac{d}{dt}\begin{pmatrix} F \\ N_k \end{pmatrix} = D^*(f^0, n_k^0)\begin{pmatrix} F \\ N_k \end{pmatrix}. \tag{15}$$

Here, D^* denotes the transposed and complex conjugated Jacobian of (13-14) evaluated along the periodic orbit (f^0, n_k^0) of (13-14). Again, we seek two solutions (F^j, N_k^j) of (15) for $j = 1, 2$ which satisfy suitable boundary and normalizing conditions. Given that these solutions have been computed, the functions

$$\Psi^j(z,t) = F^j(t)\begin{pmatrix} \Phi_-^*(z, n(t)) \\ \Phi_+^*(z, n(t)) \end{pmatrix}, \tag{16}$$

should satisfy (5-8) approximately. Upon substituting (16) into (9), the solvability conditions then read

$$\begin{aligned} \Delta\rho &= \rho_0\,\Re e\Big(e^{-i\delta}\int_0^{\frac{2\pi}{\sigma_0}} a(t-\frac{\gamma}{\sigma_0})F^1(t)^*\,\Phi_-(0,t)\,dt\Big), \\ \Delta\sigma &= \sigma_0\,\Re e\Big(e^{-i\delta}\int_0^{\frac{2\pi}{\sigma_0}} a(t-\frac{\gamma}{\sigma_0})F^2(t)^*\,\Phi_-(0,t)\,dt\Big), \end{aligned} \tag{17}$$

where δ, γ are the locked phases. If the external signal is applied to the right rather than the left facet of the laser, the solvability conditions (17) remain valid with $\Phi_-(0,t)$ replaced by $\Phi_+(L,t)$.

4 Locking properties

In this section, the method described above will be applied to the 3-section DFB laser which has been investigated in [5]. The device consists of two identical DFB sections and a passive phase-tuning section without DFB grating. Here, the phase-tuning section is located at the furthest left of the device. We listed the relevant laser parameters in Table 1. The reference frequency ω_0 corresponds to the central wavelength $\lambda = 1.57\,\mu$m. As mentioned above, this particular laser device can be modeled using the single-mode approximation described in the last section [5]. Using numerical simulations, a self-pulsating solution (f^0, n_k^0) of (13-14) is computed with parameters defined in Table 1. The temporal behavior of the output power of this free-running laser-state is shown in Fig. 1.

In order to investigate the locking properties of the free-running laser, we apply an external sinusoidal signal

$$a(t) = a_0 + a_1 e^{i\sigma t} \tag{18}$$

to the left facet of the laser. The mean power P_0 and the clock-modulated power amplitude P_{mod} of the signal are then given by $P_0 = |a_0|^2 + |a_1|^2$ and $P_{mod} = 2|a_0 a_1|$, respectively. It is worth noting that the locking region corresponding to signals of the form (18) does not depend on the phase of the coefficients a_0 and a_1. This is no longer true for more general signals. Using equation (17), the corresponding locking regions are now calculated for various values of P_0 and P_{mod}.

Firstly, we have applied the signal with a constant power ($P_{mod} = 0$) of $P_0 = 0.1\,$mW. According to (17) the locking region becomes an ellipse in the $(\Delta\rho, \Delta\sigma)$-plane. The ellipse is centered at the origin with diameters being proportional to $|a_0|$. As expected, the resonance frequencies of the laser are shifted in response to the external power.

In a second step, we perturb the SP by modulating the external power with $P_{mod} = 0.01\,$mW. This corresponds to the experimental set-up described in [6]. The locking region is shown in Fig. 2. The aforementioned ellipse is contained in the dotted area in Fig. 2 ; the locking region has therefore broadened significantly. In fact, quantitatively, we obtain locking ranges of about 0.1 nm for the wavelength and about 170 MHz for the clock frequency. This is in good agreement with experiments [6]. In addition, for a fixed pair of frequencies belonging to the locking region, there exists precisely one stable locked state.

Finally, we fix $P_{mod} = 0.01\,$mW and decrease the mean power to $P_0 = P_{mod}$. The external power is then completely modulated. The corresponding locking region is the dotted area in Fig. 3. The locking area has decreased considerably compared with the regions computed above. In addition, the fine structure in the interior of the region in Fig. 3 indicates that stable locked solutions are in general no longer unique. Indeed, for frequencies in certain subregions, there exist several stable locked states which differ by their phase offsets δ and γ. As a result, the laser may switch randomly between these states. This is certainly not desired when SP's are used for clock recovery.

For clock recovery, it seems therefore necessary to apply a relatively large background power P_0. In a real data signal, $a(t)$ will consist of many more additional components. The locking region will then experience further deformation and may become quite complicated. Even in this case, the role of the zeroth component a_0 for resonant locking is of importance.

5 Conclusions

In this article, we calculated locking regions of self-pulsating DFB lasers which are exposed to an external optical data signal. In particular, we were interested in resonant locking when both optical and power frequencies lock.

For given laser parameters, we computed the laser response for various different data signals. We showed that it is necessary to have a sufficiently large background power in order to use the laser for clock recovery. Indeed, decreasing the background power results in smaller locking regions. This behavior is in good qualitative and quantitative agreement with experiments.

It should therefore be possible to use this method as an optimization tool. For a given input signal, it is desirable to maximize the locking regions by optimizing the laser parameters for clock recovery.

References

[1] H. Wenzel, U. Bandelow, H.-J. Wünsche, and J. Rehberg, *IEEE J. Quantum Electron.* **32** (1996) 69-78.

[2] M. Möhrle, U. Feiste, J. Hörer, R. Molt, and B. Sartorius, *IEEE Photon. Technol. Lett.* **4** (1992) 976-979.

[3] B. Sartorius, M. Möhrle, and U. Feiste, *IEEE J. Select. Top. Quantum Electron.* **1** (1995) 535-538.

[4] U. Bandelow, H.-J. Wünsche, and H. Wenzel, *IEEE Photon. Technol. Lett.* **5** (1993) 1176-1179.

[5] U. Bandelow, H.-J. Wünsche,B.Sartorius, and M. Möhrle, *IEEE J. Select. Topics Quantum Electron.*, Special Issue on *Semiconductor lasers* (1997), in press.

[6] U. Feiste, D. J. As, and A. Erhardt, *IEEE Photon. Technol. Lett.* **6** (1994) 106-108.

[7] D. Peterhof, L. Recke, and B. Sandstede, in *Self-organization in activator-inhibitor systems: semiconductors, gas-discharge and chemical active media*, H. Engel et al. (eds.), Wissenschaft und Technik Verlag, Berlin, (1996) 218-222.

Figure Captions

FIG. 1 Temporal evolution of the output power of the self-pulsating laser at the left (solid line) and right (dotted line) facet of the laser. The currents are 40 mA, 131 mA and 8 mA in the phase-tuning, the middle and the right DFB-section, respectively.

FIG. 2 Locking region in $(\frac{-\lambda^2}{2\pi c}\Delta\rho, \Delta\sigma)$. Mean power and clock-modulated power amplitude are $P_0 = 0.1\,\mathrm{mW}$ and $P_{mod} = 0.01\,\mathrm{mW}$, respectively.

FIG. 3 Locking region in the same coordinates as in Fig. 2 but for a mean power of $P_0 = 0.01\,\mathrm{mW}$ and a clock-modulated power amplitude of $P_{mod} = 0.01\,\mathrm{mW}$. Compared with the results shown in Fig. 2 , the locking region has shrunk further (note that the axes are scaled differently in Figures 2 and 3).

Tables

Table 1: Parameter values used for 3-section DFB laser

	explanation	DFB section	phase-tuning section
λ	central wavelength	$1.57\,\mu\text{m}$	
r_0, r_L	facet reflectivities	10^{-6}	0.6
κ	coupling coefficient	$1.4 \cdot 10^4\,\text{m}^{-1}$	0
L_k	length	$2 \cdot 10^{-4}\,\text{m}$	$4 \cdot 10^{-4}\,\text{m}$
v_g	group velocity	$8.8 \cdot 10^7\,\text{m/s}$	$8.8 \cdot 10^7\,\text{m/s}$
β_n	differential index	$4.75 \cdot 10^{-20}\,\text{m}^2$	$7 \cdot 10^{-20}\,\text{m}^2$
g'	differential gain	$5.0 \cdot 10^{-21}\,\text{m}^2$	0
n_t	transparency concentration	$1{\cdot}10^{24}\,\text{m}^{-3}$	$3.5{\cdot}10^{23}\,\text{m}^{-3}$
α_0	internal absorption	$2500\,\text{m}^{-1}$	$4900\,\text{m}^{-1}$
β_I	thermal detuning	$50\,\text{A}^{-1}$	0
V_k	volume	$9 \cdot 10^{-17}\,\text{m}^3$	$1.8 \cdot 10^{-16}\,\text{m}^3$
τ	carrier lifetime	$2\,\text{ns}$	$1\,\text{ns}$

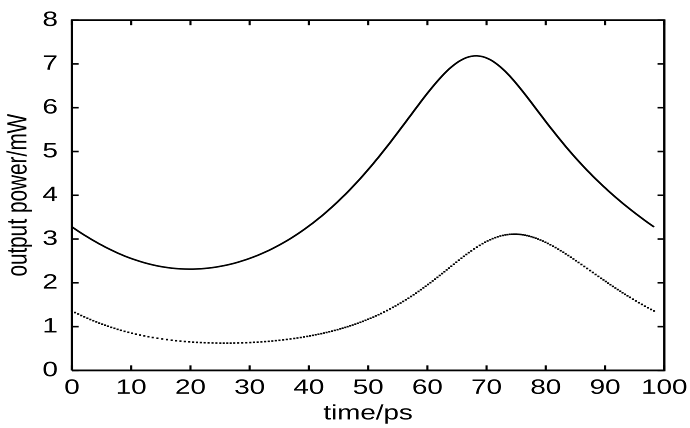

output power/mW
time/ps
0
1
2
3
4
5
6
7
8
0 10 20 30 40 50 60 70 80 90 100

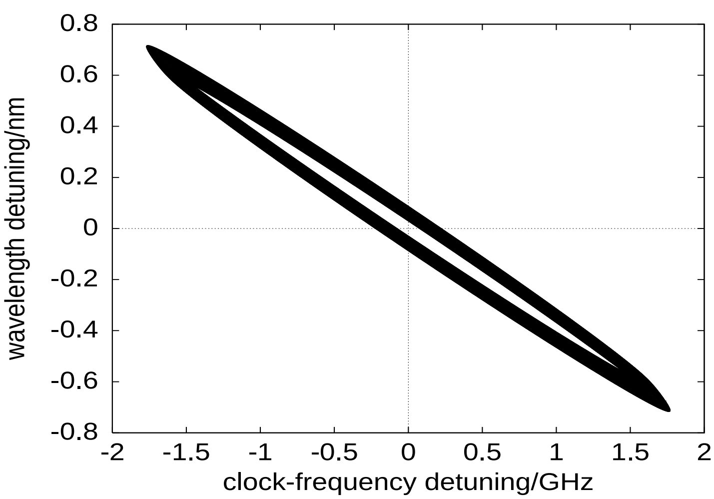
0.8
0.6
0.4
0.2
0
-0.2
-0.4
-0.6
-0.8
wavelength detuning/nm
-2
-1.5
-1
-0.5
0
0.5
1
1.5
2
clock-frequency detuning/GHz

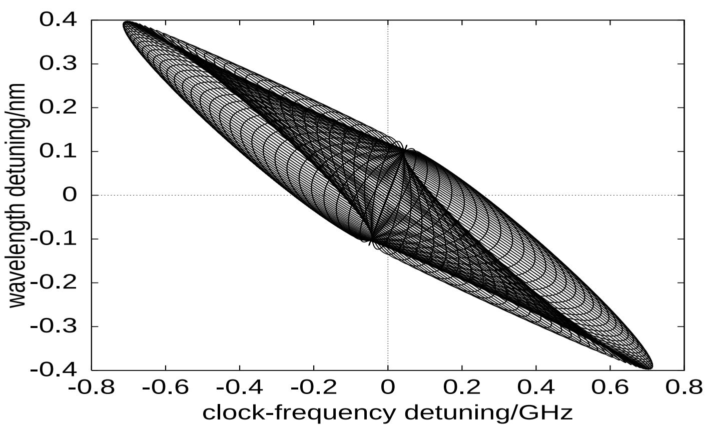
0.4
0.3
0.2
0.1
0
-0.1
-0.2
-0.3
-0.4
wavelength detuning/nm
-0.8
-0.6
-0.4
-0.2
0
0.2
0.4
0.6
0.8
clock-frequency detuning/GHz